Thermodynamics of the metal-insulator transition in the extended Hubbard model from determinantal quantum Monte Carlo

Alexander Sushchyev and Stefan Wessel◉

Institute for Theoretical Solid State Physics, RWTH Aachen University, JARA Fundamentals of Future Information Technology, and JARA Center for Simulation and Data Science, 52056 Aachen, Germany

Using finite-temperature determinantal quantum Monte Carlo simulations, we examine the thermodynamic properties of the extended Hubbard model on the half-filled square lattice in the Slater regime at intermediate coupling. We consider both the case of nearest-neighbor interactions and long-range Coulomb interactions, for coupling strengths in which the presence of nonlocal interactions still allows us to perform sign-problem free quantum Monte Carlo simulations. In particular, we assess a recently proposed scenario from variational calculations in terms of a first-order metal-insulator transition in this interaction regime.

I. INTRODUCTION

The Hubbard model [1], describing itinerant electrons in the presence of a local (on-site) repulsion, provides a most basic model to study the competition between kinetic energy and interaction effects in fermionic quantum many-body systems. A wide range of theoretical and computational approaches have been employed in order to explore its physical properties and its relevance to a wide breath of fundamental phenomena in condensed matter physics has been demonstrated, including the Mott-insulator transition, and the emergence of symmetry broken states, such as antiferromagnetism (AFM) or superconductivity (see, e.g., Ref. [2] for a recent review). This effort has contributed substantially to our current understanding of strongly correlated electron systems. Moreover, cold atom experiments provide us with a unique platform to study the physics of the Hubbard model over a wide range of controllable parameters [3].

However, in view of the fact that in solid-state materials the long-range Coulomb (LRC) interaction is only partially screened, it is important to also account for the effects of more extended interactions in addition to the local Hubbard U on the physical properties. Indeed, nonlocal interactions affect various quantities such as the electronic bandwidth [4,5], and they can induce charge density wave states [6–10], to name but a few consequences.

Recently, the effects of nonlocal interactions on the metal-insulator transition on the half-filled square lattice have been explored, based on a variational approach [11,12]. More specifically, by means of the Peierls-Feynmann-Bogoliubov variational principle, the extended Hubbard model was approximated in Ref. [12] by an effective (local) Hubbard model in terms of an effective hopping parameter and local interaction strength $\tilde{U}$. For this purpose, the variational free energy was calculated based on the integration of thermodynamic data for the effective (local) Hubbard model, obtained using determinantal quantum Monte Carlo (DQMC) simulations on a dense parameter grid, applying a two-dimensional Savitzky-

Golay filter and spline interpolation to the grid data [12]. Based on this variational approach, several conclusions regarding the effects of nonlocal interactions were drawn. In particular, two distinct mechanisms are described in Ref. [12], how nonlocal interactions suppress correlation effects: Within the Fermi-liquid regime they reduce $\tilde{U}$, while they increase the effective hopping strength within the insulating regime. Moreover, the competition between both mechanisms was found to drive a first-order metal-insulator transition in the presence of nonlocal interactions. From a comparison of the associated entropy jump across the transition with available experimental data on materials with purely electronic metal-insulator transitions, the authors conclude that nonlocal interactions are at least in part responsible for the discontinuous metal-insulator transitions observed in correlated electron materials. In view of the above, it is mandatory to compare the results from the variational approach to unbiased calculations that take the nonlocal interactions fully into account. In fact, as noted in Ref. [12], the parameter region in which the discontinuous thermodynamic behavior was observed is accessible to sign-problem free DQMC simulations, i.e., including a full treatment of the nonlocal interaction terms [13,14].

Here we report results from unbiased DQMC simulations of the extended Hubbard model in order to assess the qualitative and quantitative appropriateness of the variational approach [12]. In particular, we probe for unbiased evidence for the emergence of the discontinuous thermodynamic behavior reported in Ref. [12] as a result of nonlocal interactions. The remainder of this paper is organized as follows: In Sec. II we define the extended Hubbard models that we consider here, and also specify our computational approach. The results obtained from our DQMC calculations are then reported in Sec. III, and final conclusions are given in Sec. IV.

II. MODEL AND METHOD

In the following we consider the extended Hubbard model with nonlocal density-density interactions, described by the

Hamiltonian

$$H = -t \sum_{\langle i,j \rangle, \sigma} (c_{i\sigma}^\dagger c_{j\sigma} + \text{H.c.}) + U \sum_i n_{i\uparrow} n_{j\downarrow} + \frac{1}{2} \sum_{i \neq j} V_{ij} n_i n_j$$

(1)

on the square lattice. Here $c_{i\sigma}^\dagger$ ($c_{i\sigma}$) denotes the creation (annihilation) operator for electrons on site i with spin projection σ, $n_{i\sigma} = c_{i\sigma}^\dagger c_{i\sigma}$ the local spin-resolved occupation operators, and $n_i = n_{i\uparrow} + n_{i\downarrow}$ the total local occupation. Furthermore, t denotes the nearest-neighbor hopping amplitude, U the local (Hubbard) repulsion, and V_{ij} the nonlocal interaction between electrons on site i and j. In the following we will focus on two different cases: (i) the so-called U-V model with nearest-neighbor interactions of strength V, and (ii) LRC interactions with $V_{ij} = V_C/d_{ij}$, where d_{ij} denotes the distance between sites i and j (the lattice constant $a = 1$). In all our investigations, we consider the case of half-filling.

In order to examine the thermodynamic properties of the above model, we use DQMC simulations [15], performed using the ALF code [16]. This allows us to simulate the above model sign-problem free using appropriate Hubbard-Stratanovich decoupling schemes [13,14] for both the on-site and nonlocal interactions within the regimes (i) $V \leqslant U/4$ for the U-V model, and (ii) $V_C \lesssim 0.62U$, such that $U\delta_{ij} + V_{ij}$ is a positive-definite matrix, for the LRC-Hubbard model case. Note that an earlier DQMC work on the U-V extended Hubbard model used a decoupling scheme that leads to a sign problem for any finite $V > 0$ [7] (this fact is not mentioned explicitly in that reference). For the DQMC simulations, we consider finite square lattices with $N = L \times L$ lattice sites with periodic boundary conditions in both lattice directions and the standard minimum image convention for the case of LRC interactions. We denote the (inverse) temperature by T ($\beta = 1/T$) in the following ($k_B = 1$).

In our analysis, we mainly concentrate on DQMC results for the double occupancy,

$$D = \frac{1}{N} \sum_{i=1}^N \langle n_{i\uparrow} n_{i\downarrow} \rangle,$$

(2)

for which we perform a spatial averaging in order to enhance the statistical accuracy. We also draw attention to a recent proposal on how to improve the DQMC sampling procedure in order to further reduce statistical fluctuations on such local quantities [17]. For the DQMC simulations a Trotter decomposition of H is used with a small imaginary-time step $\Delta\tau$. For the reported DQMC results for D, we preformed a $\Delta\tau \to 0$ extrapolation, as detailed in Appendix A, and the data shown below has always been obtained from this analysis. Furthermore, we report results for the entropy S (per site), which we obtain from the DQMC values of the internal energy E (per site) at $\Delta\tau = 0.1/t$ via thermodynamic integration,

$$S(\beta) = \beta E(\beta) + \ln(4) - \int_0^\beta E(\beta') \, d\beta'.$$

(3)

The integral is evaluated numerically using the trapezoidal rule on a dense β mesh. In addition to these thermodynamic quantities, we also measured in the QMC simulations the structure factors for AFM, stabilized, e.g., in the ground state
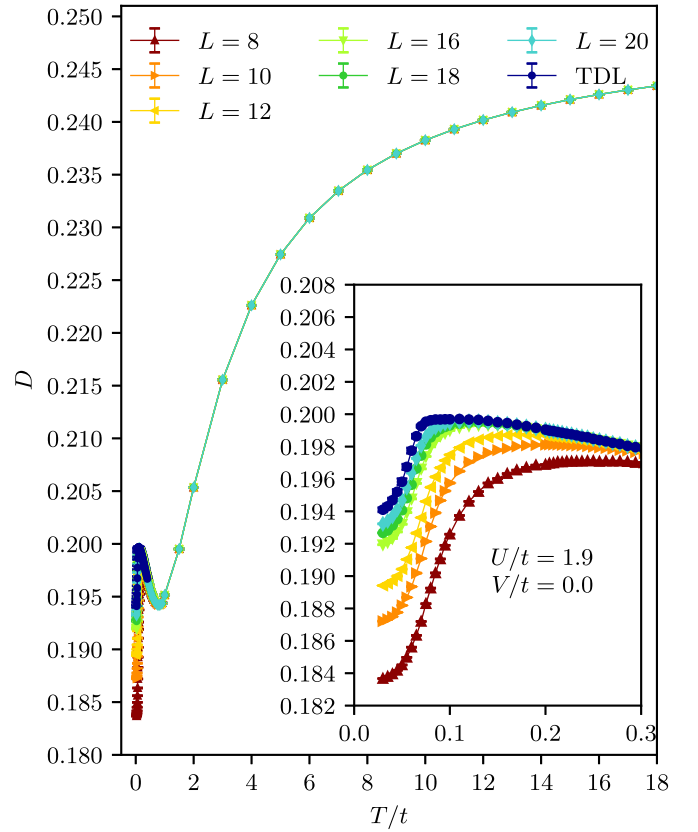

FIG. 1. Temperature dependence of the double occupancy D for the Hubbard model at $U/t = 1.9$. The inset focuses on the low-temperature regime containing the local maximum.

of the Hubbard model at half-filling,

$$S_{\text{AF}} = \frac{1}{N} \sum_{i,j=1}^N \varepsilon_i \varepsilon_j \langle \mathbf{S}_i \cdot \mathbf{S}_j \rangle,$$

(4)

as well as for the commensurate charge density wave (CDW) state that is expected to be stabilized for sufficiently strong V in the U-V model [7],

$$S_{\text{CDW}} = \frac{1}{N} \sum_{i,j=1}^N \varepsilon_i \varepsilon_j \langle n_i n_j \rangle.$$

(5)

Here $\varepsilon_i = \pm 1$, depending on which sublattice the site i belongs to on the bipartite square lattice.

III. RESULTS

In this section we report results from DQMC simulations and compare them with previously reported findings. Before we consider the case of nonlocal interactions, we first present DQMC results for the Hubbard model (i.e., $V = V_C = 0$).

A. The Hubbard model

While highly accurate and detailed DQMC results of various thermodynamic quantities for the Hubbard model has been reported in Ref. [18], these do not include the thermal behavior of both D and S, which we report below. In order
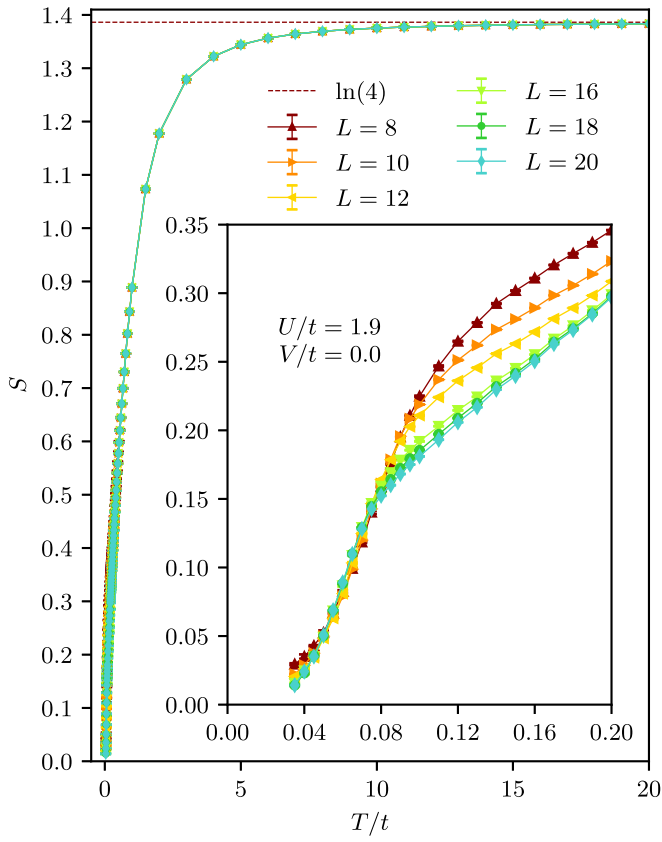
FIG. 2. Temperature dependence of the entropy S for the Hubbard model at $U/t = 1.9$. The inset focuses on the low-temperature regime.

to allow for a direct comparison to the numerical results reported from the variational approach in Ref. [12], we focus in the following on the specific parameter ratio $U/t = 1$.
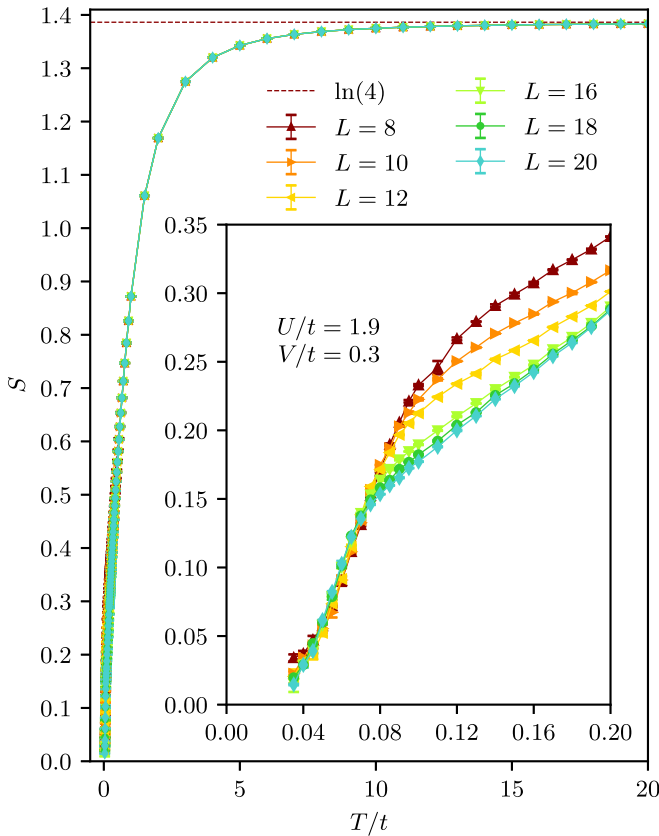
FIG. 4. Temperature dependence of the entropy S for the U-V model at $U/t = 1.9$, $V/t = 0.3$. The inset focuses on the low-temperature regime.

FIG. 5. Temperature dependence of the TDL-extrapolated double occupancy D (top panel) and the entropy S for the $L = 20$ systems (middle panel) for the considered models with $U/t = 1.9$, for $V/t = 0.3$ and $V_C/t = 1.9$, respectively. The bottom panel shows the difference $S - S_0$ of the entropy for the models with extended interactions with respect to the entropy of the Hubbard model (denoted S_0 here).

Before we turn to nonzero values of V, we briefly report the DQMC results for the entropy S for the same value of $U/t = 1.9$, cf. Fig. 2. In the intermediate temperature regime below about $T \approx t$, we observe an essentially linear decrease of S for large systems, down to a temperature of $T \approx 0.08t$. At lower temperatures, the entropy decreases more rapidly with decreasing temperature. Overall, this behavior matches the aforementioned similar asymmetric drop in D near its local maximum at $T_{\max}$. The enhanced reduction of both D and S below $T_{\max}$ reflects the Stoner effect mentioned above upon entering the regime where AFM fluctuations proliferate. In the finite-size data of the entropy we furthermore identify a small temperature window below $T_{\max}$, in which S exhibits a (mild) increase with system size L, in contrast to its decrease with increasing L outside of this regime. A possible explanation for the anomalous behavior is the growth of the AFM correlation length on scales comparable to the simulated system sizes in this regime. By contrast, for lower (higher) temperatures, the correlation length instead resides well beyond (below) the finite size of the simulation cell.

B. The U-V model

We next turn to the U-V model, and consider in particular a value of $V/t = 0.3$, again for $U/t = 1.9$. Namely, for this value of V a noticeable jump in D was observed within the variational approach at a temperature of $T \approx 0.085t$, and was taken as indication of a first-order metal-insulator transition
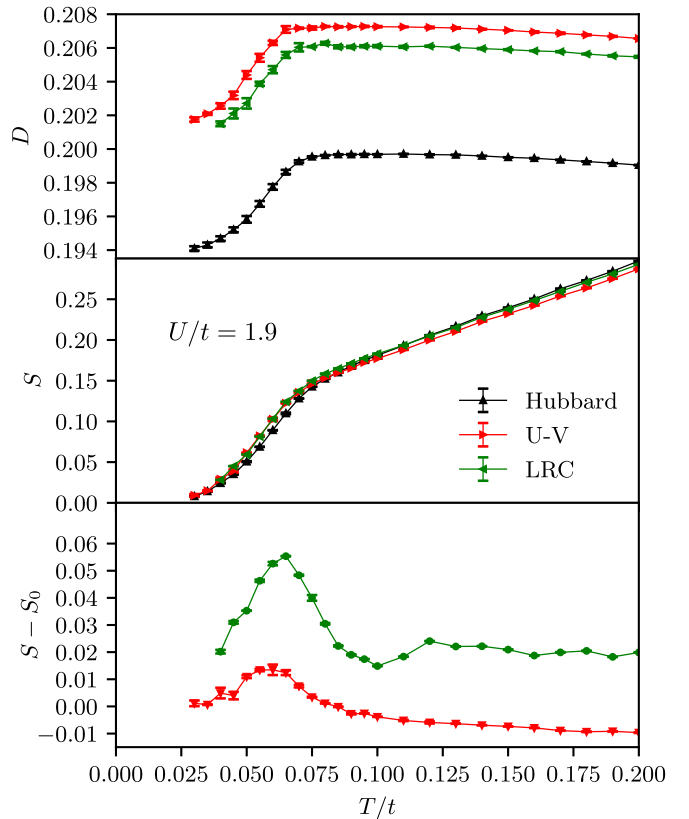
[12]. Performing the data analysis as in the previous section, we obtain the DQMC results shown in Figs. 3 and 4 for D and S, respectively. For the purpose of a direct comparison, the QMC data for both D and S for the different models are also collected in Fig. 5. In agreement with general expectations and the results from the variational approach, we observe an increase of D for the case of finite V as compared to the $V = 0$ case, corresponding to an overall decrease of the local correlations. Correspondingly, we also observe a mild enhancement of the entropy in the low-temperature region for finite $V > 0$, while otherwise S also shows a behavior similar to the one at $V = 0$. Besides the overall increase in the values of D, we observe no significant change in, e.g., the temperature of the maximum in D.

In contrast to the variational approach, the finite-size DQMC data does not exhibit any indication for the onset of a discontinuity in D near the local maximum. We do observe in the TDL extrapolation a somewhat steeper drop of D on the low-temperature side of the maximum than for $V = 0$, but no indication for a jump is obtained. It was already noted in Ref. [12] that the discontinuity obtained within the variational approach is of order 3×10^{-4} for $V/t = 0.3$ and thus actually rather small. On the other hand, we noted already for the case $V = 0$, discussed in the previous section, that the values for D
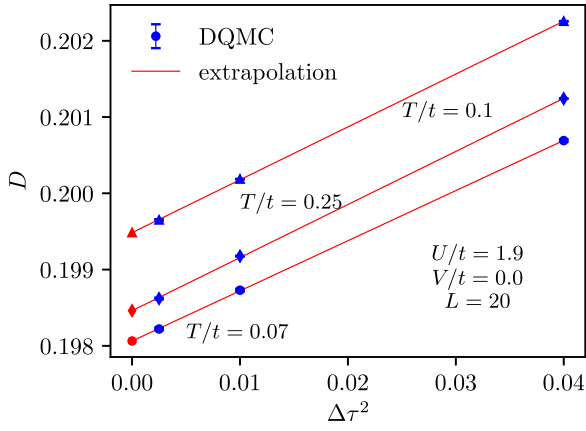
0

FIG. 12. Trotter-discretization extrapolation of the double occupancy D for the Hubbard model at $U/t = 1.9$, $L = 20$, for different values of the temperature T.

APPENDIX B: FINITE-SIZE EXTRAPOLATION

In order to extrapolate the finite-size DQMC data to the TDL, we need to account for the leading finite-size correction at low temperatures in terms of a finite (correlation) length scale from thermal fluctuations. In particular, for the double occupancy, the TDL value D_{TDL} is obtained by fitting the finite-size data D (as obtained from performing the $\Delta\tau \to 0$